Journal of Molecular Catalysis A: Chemical 305 (2009) 34–39

Contents lists available at ScienceDirect

Journal of Molecular Catalysis A: Chemical

journal homepage: www.elsevier.com/locate/molcata

Zeolite synthesis in presence of hexamethonium ions

G. Giordano [a,*], J.B. Nagy [a], E.G. Derouane [b,1]

[a] Dipartimento di Ingegneria Chimica e dei Materiali, Università della Calabria, I-87030 RENDE (CS), Italy
[b] University of Algarve, Faro, Portugal

ARTICLE INFO

Article history:
Available online 9 January 2009

Keywords:
ZSM-48
EU-1 zeolite synthesis
Crystallization fields
Pore filling
^{13}C NMR

ABSTRACT

The role played by hexamethonium ions in the synthesis of one-dimensional ZSM-48 and EU-1 zeolitic structures is investigated. A systematic study is carried out to determine the factors influencing the preferential crystallization and/or co-crystallization of ZSM-48 and EU-1 from a sodium–hexamethonium–silica–alumina hydrogel. The influence of sodium and organic content and the Si/Al ratio in the initial hydrogel is specifically examined. An explanation is proposed for the accommodation of the hexamethonium ions in the different zeolitic frameworks of ZSM-48 and EU-1.

1. Introduction

The present study is devoted to the investigation of the role played by hexamethonium ions in the synthesis of ZSM-48 and EU-1 zeolites that were described in patents by Casci et al. [1,2]. The importance of the diquaternary ammonium ions in the zeolite synthesis from a hydrogel to obtain new zeolitic frameworks has been underlined in the literature [3,4].

The diquaternary ammonium ions address a series of one-dimensional zeolite frameworks, such as EUO, MTN, MTT, MTW, EU-4 and ZSM-48 type structure [1–7] and probably they play a pore filling and stabilizing role of the zeolitic framework.

Indeed, with the same template, diversities of high-silica zeolite structures can be obtained and a specific structure can often be crystallized in presence of a variety of templates [4,8].

In the last decade, the literature has reported a new two-dimensional zeolite structure NES, and a multi-dimensional Nu-86 type obtained by using diquaternary ammonium ions [6,9]. The aforesaid one-dimensional zeolites show interesting properties in adsorption processes, especially by their hydrophobic Si-rich forms, and also in catalytic application, such as the isopropylation of benzene over EUO type zeolite catalyst [10].

The interest in the zeolite type formed in presence of hexamethonium ions such as ZSM-48 and EUO type is due to the different catalytic properties shown by this kind of zeolitic framework. The ZSM-48 shows very interesting properties in FCC processes. As a matter of fact the addition of the ZSM-48 (5 or 10 wt.%) to the USY catalyst gives an increase in the conversion (3 points) and in the total gas fraction (10 points) and a decrease in the residual (about 2 points) [11]. In addition, the presence of ZSM-48 increases the formation of C_3 and C_4 olefins. The EUO type zeolite shows interesting application in isomerization of aromatics [12–14] and in the production of 2,6-dimethylnaphthalene [15]. The molecular shape selectivity of EUO was discussed showing the importance of the sitting of Al in the framework [16].

The structure of EU-1 zeolite was also investigated by neutron diffraction [17]. A thermodynamic study of cation exchange in EU-1 was also reported [18]. Intracrystalline diffusion of linear and branched alkanes [19] and EU-1 as hydrocarbon traps were also investigated [20].

Of course, it is possible to obtain some of these zeolite structures using many different organic molecules in a large range of composition and in different media [21–27]. The literature reports also the possibility of the partial or complete isomorphous substitution of Al with other metals [28–32]. Very often EU-1 and ZSM-48 zeolites co-crystallize when hexamethonium ions are used. The effect of both the presence of alkali cations and the presence of aluminium was examined on the formation of ZSM-48 zeolites. To better approach the role the organic molecules play in zeolite synthesis, several organic molecules can be used in competition. The specific formation of Silicalite-1, Silicalite-2 and ZSM-48 could be favoured from batch containing tetraalkylammonium bromide, hexamethonium bromide and diaminodecane, in presence of fluoride ions [33]. It was also shown that layered organic–inorganic compounds are formed during the crystallization of ZSM-48 with hexamethonium ions [34]. Interestingly it was also shown that these layered compounds are not true intermediates in zeolite synthesis and they only provide the synthesis medium with silicate and aluminosilicate species necessary for the crystallization of the particular zeolite.

* Corresponding author.
E-mail address: ggiorda@unical.it (G. Giordano).
[1] Deceased.

1381-1169/$ – see front matter © 2008 Elsevier B.V. All rights reserved.
doi:10.1016/j.molcata.2008.12.024

The structure of the latter is directed by the organic species present in solution [34,35].

Very interesting results were reported by Casci on the role played by hexamethonium in the EU-1 synthesis [6]. At high hexamethonium content in the reaction mixture EU-1 zeolite is obtained preferentially. However, when only catalytic amount of HM ions are used, no MFI type zeolite is obtained, although without hexamethonium this zeolite is the preferred product. The role of the catalytic amount of HM ions was ascribed to a structure blocking effect of the MFI nuclei [6].

Emphasis was also put on the accommodation of the organic template in the channel and the side-pocket of the EUO structure. Molecular modelling was essentially used to propose the position of HM ions: they are situated in the 12-member ring side-pocket and are perpendicular to the main channel formed by 10-membered rings [35–37].

Following these literature suggestions and with the aim of a better understanding of the role played by hexamethonium ions in the formation of ZSM-48 and EUO type structures, we have systematically investigated the hydrogel systems

$$x\mathrm{Na_2O}–y\mathrm{HMBr_2}–0.5\mathrm{Al_2O_3}–w\mathrm{SiO_2}–3000\mathrm{H_2O}$$

(where $HMBr_2$ stands for hexamethonium bromide) in a large composition range. The investigation has been carried out especially in the Si/Al ratios when zeolites ZSM-48 and EU-1 co-crystallize; also the amount of HM^{2+} ions in hydrogel has been varied for a better understanding of the pore filling role that they play in the different zeolite frameworks.

Finally, a model for the location of HM^{2+} ions in the ZSM-48 and EU-1 zeolitic structure is proposed.

2. Experimental

2.1. Synthesis

A series of hydrogels having the following molar composition:

$$x\mathrm{Na_2O}–y\mathrm{HMBr_2}–0.5\mathrm{Al_2O_3}–w\mathrm{SiO_2}–3000\mathrm{H_2O}$$

was prepared (x ranging from 3 to 12, y from 2.5 to 20 and w from 5 to 75) by mixing high purity reactants in the following order: aluminium hydroxide (Aldrich), sodium hydroxide (Carlo Erba RPE), distilled water, hexamethonium bromide (Aldrich) and fumed silica (fumed, Aerosil Serva). After homogenization, the hydrogels were transferred into 20 ml Teflon-lined Morey-type reactors and heated at $190 \pm 2\,^{\circ}C$ in static condition and under autogeneous pressure for a period varying from 1 to 11 days. After thermal treatment, the reactors were removed from the oven and the reaction was quenched by cooling down to room temperature in cold water. The reaction products were filtered, thoroughly washed with distilled water and dried overnight at 105 °C.

2.2. Characterization

All the samples were examined by X-ray powder diffraction (XRD) (Philips PW 1730/10 X-ray generator equipped with a PW 1050/70 vertical goniometer, Cu $K\alpha_1$ radiation) to identify the solid phases. Before analysis, the crystalline phases of all the samples were enriched by ultrasonic treatment that removed the residual amorphous phases. The amount of water and organic molecules was evaluated by thermal analysis (Netzsch STA 409 combined TG-DTG-DSC thermoanalyzer). Sodium, aluminium and silica content were determined by energy-dispersive X-ray analysis (EDX) (Jeol SEM T330 equipped with Tracor Northern EDX). The NMR analysis was carried out on a Bruker CXP 200 spectrometer at 50.3 MHz. The CP conditions were: $\pi/2$ pulse = 5 μs, contact time = 5 ms and repetition time = 4.0 s. The magic angle spinning was at 3.5 kHz with a zirconia rotor. Three thousand free induction decays were accumulated before Fourier transformation.

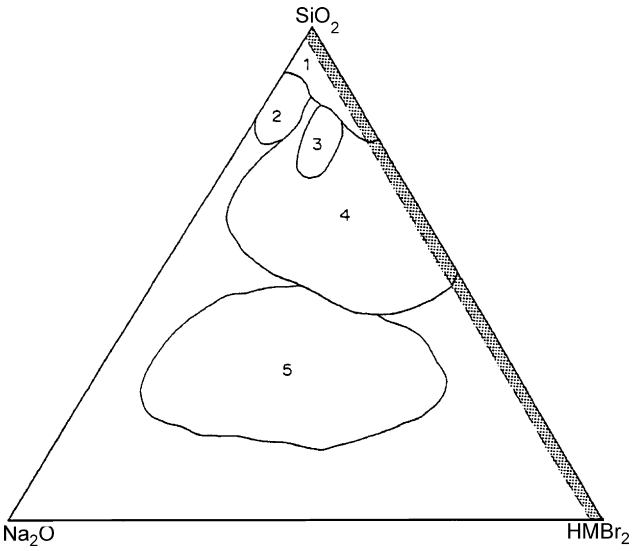

Fig. 1. Ternary diagram of the solid phases obtained after 7 days of hydrothermal treatment at 190 °C of the hydrogel: $x\mathrm{Na_2O}–y\mathrm{HMBr_2}–0.5\mathrm{Al_2O_3}–w\mathrm{SiO_2}–3000\mathrm{H_2O}$; 1 = ZSM-48; 2 = ZSM-48 + EU-1 + quartz; 3 = ZSM-48 + EU-1; 4 = EU-1; 5 = Analcime, in shadow not explored area.

3. Results and discussion

Generally the Si/Al ratio influences the formation of secondary building units (SBU). For example, a preliminary investigation of the starting hydrogel without organic molecules has confirmed the formation of simpler SBU in a low Si/Al range leading to ANA type zeolite. Inaoka et al. have demonstrated that medium Si/Al ratios lead to the formation of 5-1 SBU such as MFI type or MOR type structures, while high Si/Al ratios favour the co-crystallization of quartz with 5-1 SBU [38].

Fig. 1 shows the crystallization field of the different solid phases obtained from the hydrogels containing hexamethonium ions. Analcime is the only product for a low Si/Al ratio equal to 5. This confirms that the presence of organic molecules does not have a strong influence on the Al-rich hydrogel to address the reaction mixture to a preferential structure, but the sodium content, the Si/Al ratio and the synthesis temperature influence essentially the reaction products.

On the other hand, it is evident that the EU-1 zeolite has a large crystallization range (region 4) compared with the ZSM-48 zeolite (region 1), which presents a smaller crystallization field. The field of co-crystallization of the ZSM-48 and EU-1 zeolites (region 3), containing also dense phases (region 2), shows a small formation area compared with that of EU-1. In particular, EU-1 is the main product for Si/Al ratio equal to 25 and ZSM-48 for Si/Al ratio equal to 75.

The OH^- content is responsible, first of all, for the solubility of silica and aluminium species and consequently for the crystallization rate and yield, secondly it favours the formation of dense phases such as quartz in Si-rich and HM^{2+} poor hydrogel systems.

The Si/Al ratio of 50 leads to a co-crystallization of ZSM-48 and EU-1 zeolites. Table 1 reports the crystallinity of the so-formed zeolitic phases ZSM-48 and EU-1. First of all, it can be observed that for a high amount of HM^{2+} ions in the starting hydrogel (samples 17–20) quartz is not found in the reaction products. Traces of quartz are detected only in Si-rich hydrogels when it co-crystallizes with ZSM-48 and EU-1.

Table 1
Crystallinity phases of so-formed ZSM-48 and EU-1 obtained from the system: xNa_2O–$yHMBr_2$–$0.5Al_2O_3$–$wSiO_2$–$3000H_2O$, after a hydrothermal treatment of 7 days at 190 °C.

Sample	Mole	in	Hydrogel	Crystalline phase detected by X-ray and SEM
	x	*y*	*w*	
1	3	2.5	25	[Amorphous] + EU-1 traces
2	6	2.5	25	EU-1
3	9	2.5	25	[EU-1] + amorphous
4	12	2.5	25	[EU-1] + amorphous
5	3	2.5	50	[Amorphous] + ZSM-48 + EU-1 traces
6	6	2.5	50	[ZSM-48] + EU-1
7	9	2.5	50	[EU-1] + ZSM-48 + quartz
8	12	2.5	50	[EU-1] + ZSM-48
9	3	2.5	75	ZSM-48
10	6	2.5	75	ZSM-48
11	9	2.5	75	[ZSM-48] + EU-1 traces
12	12	2.5	75	[ZSM-48] + EU-1 traces + quartz
13	3	10	25	[EU-1] + ZSM-48 traces
14	6	10	25	EU-1
15	9	10	25	EU-1
16	12	10	25	EU-1
17	3	10	50	[ZSM-48] + EU-1 traces
18	6	10	50	[EU-1] + ZSM-48
19	9	10	50	[EU-1] + ZSM-48
20	12	10	50	[EU-1] + ZSM-48
21	3	10	75	[ZSM-48] + amorphous
22	6	10	75	ZSM-48
23	9	10	75	[ZSM-48] + EU-1 traces
24	12	10	75	[ZSM-48] + EU-1 traces + quartz

In the case of co-crystallization in brackets is reported the main phase observed.

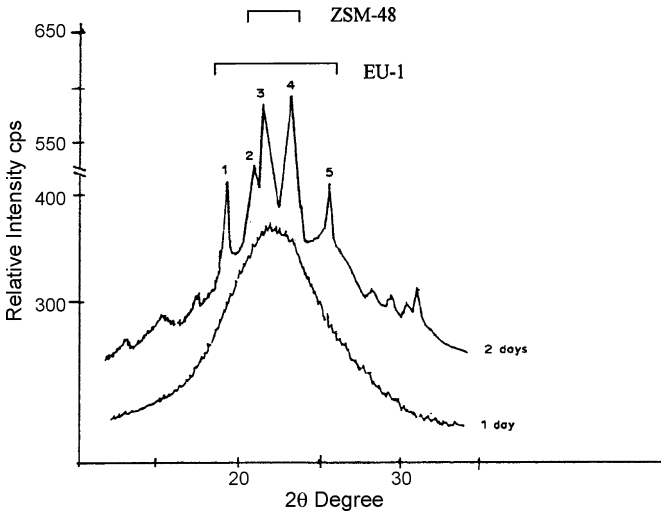

Fig. 2. X-ray diffraction patterns of the synthesis no. 6 (see Table 1), stopped at 1 and 2 days. 1, 2 and 5 main peaks of EU-1. 3 and 4 main peaks of ZSM-48.

Secondly, it is manifest that a large amount of hexamethonium ions is unfavourable for a good crystallization of ZSM-48 zeolite, and for high Al content the formation of EU-1 is favoured [33]. Consequently the pure ZSM-48 zeolite formation is favoured in a hydrogel containing only a small amount of HM^{2+} for OH^-/SiO_2 ratios varying between 0.08 and 0.16 and EU-1 in a rich HM^{2+} ions media for OH^-/SiO_2 ratios ranging from 0.48 to 0.96. In fact, a larger amount of sodium hydroxide accelerates the growth of Al-rich phases, EU-1 for Si/Al = 25, and Analcime for Si/Al = 5 and OH^-/SiO_2 ratio higher than 1.

The aluminium content in the hydrogel influences the formation of different zeolitic phases. Indeed, a higher amount of Al favours the crystallization of Analcime, the medium content the formation of EU-1 and a low Al content is advantageous for the crystallization of ZSM-48 zeolite (Fig. 1).

From an X-ray diffractogram analysis (see Fig. 2) of the synthesis stopped at different crystallization times (Si/Al = 50 in the hydrogel) it can be seen that a concomitant co-crystallization of ZSM-48 and EU-1 occurs from the starting hydrogel. This occurs for both hydrogels poor and rich in HM^{2+} ions, and hence it is the Si/Al ratio, which influences the formation of either the silica-rich ZSM-48 or the EU-1 zeolite having a higher Al content.

The influence of the amount of HM^{2+} ions is shown in Fig. 3a and b, where are reported the X-ray diffractograms of two different systems with the same Si/Al ratio equal to 50 and OH^-/SiO_2 equal to 0.36. The first one (Fig. 3a), with 2.5 moles of hexamethonium ions, the second one (Fig. 3b), with 10 moles. Fig. 3a shows, that after 11 days of synthesis ZSM-48 is transformed into quartz, whereas the amount of EU-1 increases. By contrast (Fig. 3b), the same hydrogel with 10 moles of hexamethonium ions shows a stability of the so-formed zeolitic phases, even for a long synthesis time, 9 days, while for the same reaction time, in systems containing only a small amount of HM^{2+} ions (see Fig. 3a) quartz appears clearly. This can be explained by considering that the ZSM-48 is a Si-rich zeolite. In a system involving a crystallization competition, the Al-rich phases (EU-1 in this case) are attracting more HM^{2+} ions to stabilize both the $[Si–O–Al]^-$ negative charges [33] and this particular framework (for ZSM-48: $HM^{2+}/u.c. \approx 1$, $HM^{2+}/Al + Si \approx 0.021$; for EU-1: $HM^{2+}/u.c. \approx 4$, $HM^{2+}/Al + Si \approx 0.036$, see below).

On the other hand, it is known that, for a low amount of HM^{2+} ions in the hydrogel and at a synthesis temperature of 200 °C, the ZSM-48 zeolite co-crystallizes with dense phases [21,25], because in this case the ZSM-48 framework cannot be well filled by the organic molecules. By contrast, in a HM^{2+} ions rich system, the amount of organic molecules is sufficient to fill and stabilize both zeolitic structures, and consequently the dense phases do not appear at the temperature examined. This observation confirms the metastability of ZSM-48 zeolite in a low HM^{2+} medium.

Fig. 4 shows the percentage of crystallinity of EU-1 zeolite as a function of the OH^-/HM^{2+} ratio for a Si/Al ratio equal to 25. One can see that the maximum of crystallinity is obtained for a OH^-/HM^{2+} ratio close to 1, therefore for a larger amount of HM^{2+} ions in the starting hydrogel.

Finally, the optimum parameters for the ZSM-48 zeolite synthesized in the alkali-hexamethonium system is a high Si/Al ratio from 75 to ∞, a OH^-/SiO_2 ratio between 0.08 and 0.16 and a OH^-/HM^{2+} ratio between 2.5 and 5. For a rapid and efficient EU-1 synthesis we suggest the following ratios: Si/Al close to 25, OH^-/SiO_2 between 0.48 and 0.96 and OH^-/HM^{2+} close to 1. The synthesis of ZSM-48 zeolite is thus favoured in absence of Al [21,33,34] and in a relatively poor OH^- and HM^{2+} ions medium. By contrast, EU-1 formation prefers a medium Si/Al ratio and a high content of the OH^- and HM^{2+} ions.

In Table 2 are reported the chemical analyses of different ZSM-48 and EU-1 zeolites. The results relative to the ZSM-48 are in good agreement with previous observations [21,33], that in all cases only a small amount of sodium per unit cell is incorporated into the framework. So the neutralizing role of HM^{2+} ions of the $[Si–O–Al]^-$ negative charges is clearly confirmed. Generally, the amount of Al per unit cell is close to or less than 1 [35]. The low value of the water per unit cell incorporated into the zeolitic framework confirms the hydrophobicity of the ZSM-48 and of the high-silica zeolites. The organic content per unit cell close to 1 is sufficient to assure a good pore filling of the intracrystalline ZSM-48 volume. Indeed, the estimated length of hexamethonium is 14.5 Å and it is close to the channel length of one unit cell of ZSM-48 equal to 16.8 Å.

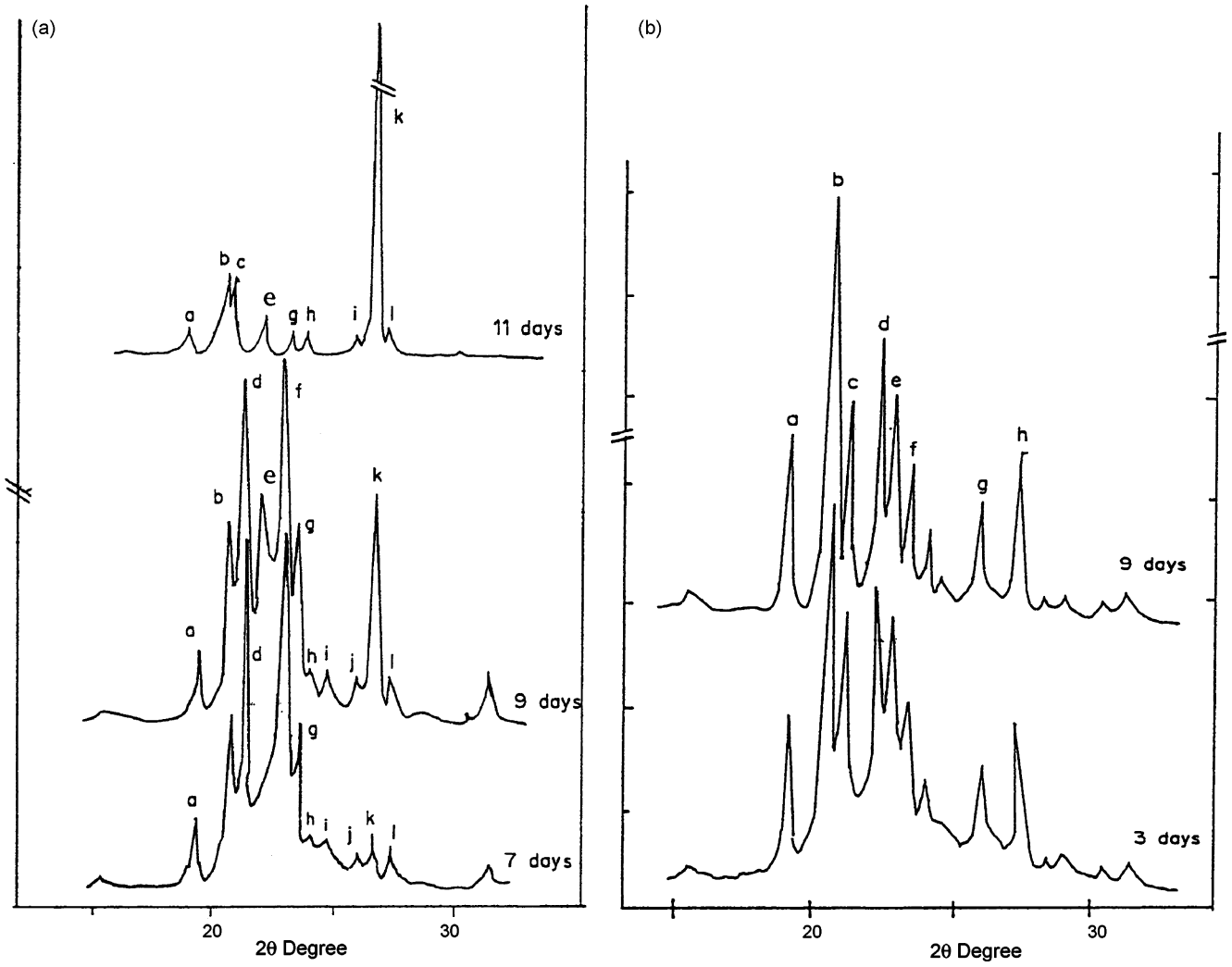

Fig. 3. (a) X-ray patterns of the synthesis no. 7 (see Table 1) stopped at 7, 9 and 11 days. a, b, g, h, i, j and l peaks of EU-1. d and f peaks of ZSM-48. e peak of cristobalite. c and k peaks of quartz. (b) X-ray patterns of the synthesis no. 19 (see Table 1) stopped at 3 and 9 days. a, b, d, f, g and h peaks of EU-1. c and e peaks of ZSM-48.

On the other hand, the EU-1 zeolite, compared with ZSM-48 shows a larger incorporation of sodium, aluminium and hexamethonium per unit cell. In all samples the Al content per unit cell is higher than 4, confirming that the EUO structure is able to accommodate a larger amount of Al compared with other Si-rich zeolites. The sodium content per unit cell is less than that required to completely neutralize the framework $[Si–O–Al]^-$ negative charges. This means that the HM^{2+} ions also act as counterions to framework

Table 2
Chemical composition of various ZSM-48 and EU-1 zeolites.

Sample	Zeolitic phases	H_2O/u.c.[a]	HM^{2+}/u.c.[a]	Na/u.c.[b]	Al/u.c.[b]	Pore filling[c]
10	ZSM-48	1.6	0.9	0.3	0.9	78
21	ZSM-48	1.2	0.8	0.2	0.7	61
				0.2 (ZSM-48)	0.8 (ZSM-48)	
7	[EU-1] + ZSM-48	2.2				
				1.1 (EU-1)	4.1 (EU-1)	
				0.3 (ZSM-48)	0.3 (ZSM-48)	
19	[EU-1] + ZSM-48	2.4				
				1.5 (EU-1)	1.5 (EU-1)	
27[d]	EU-1	3.0	4.1	1.2	4.7	
28[d]	EU-1	3.2	4.0	1.4	4.8	
31[e]	EU-1	3.0	4.3	1.2	4.5	
32[e]	EU-1	3.2	4.3	1.6	4.5	

In brackets main product detected.

[a] Water and organic content was determined by TG-DTG-DSC analysis.

[b] Sodium and aluminium content was evaluated by EDX analysis as an average of 5 analyses of single crystals.

[c] Pore filling percentage was calculated by considering the total channel length of one ZSM-48 unit cell equal to 16.8 Å and the length of HM^{2+} equal to 14.5 Å. The length of HM^{2+} ions has been estimated by considering the following bond distances: C–C = 1.541 Å; C–N = 1.479 Å; C–H = 1.101 Å; N–H = 1.000 Å; van der Waals radius of hydrogen = 1.200 Å and tetrahedral angle = 109°.

[d] Synthesis 27 and 28 are from system: $x Na_2O–15HMBr_2–0.5Al_2O_3–25SiO_2–3000H_2O$ with 9 and 12 Na_2O, respectively.

[e] Synthesis 31 and 32 are from system: $x Na_2O–20HMBr_2–0.5Al_2O_3–25SiO_2–3000H_2O$ with 9 and 12 Na_2O, respectively.

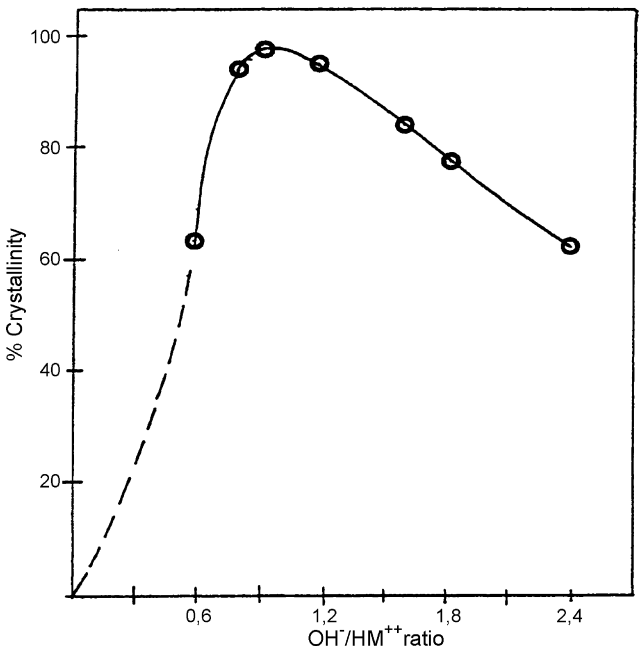

Fig. 4. Crystallinity % of EU-1 synthesized from the system: xNa$_2$O–yHMBr$_2$–0.5Al$_2$O$_3$–25SiO$_2$–3000H$_2$O as a function of OH^-/HM^{2+} ratio.

negative charges. The hexamethonium per unit cell observed is close to 4. The values of sodium and aluminium detected in the case of co-crystallization of ZSM-48 with EU-1 (samples 7 and 19, Table 2) do confirm the different sodium, aluminium and HM^{2+} content in these zeolites.

Finally, in the case of ZSM-48 type structure it is clear that the hexamethonium ions are incorporated in the linear channel of the zeolite. The chemical analyses evidence this proposition. Indeed the length of one HM^{2+} ion is close to the total length of one ZSM-48 unit cell, and in all the analyses we observe about 1 HM^{2+} per unit cell (see also Refs. [31,33]). On the other hand, the amount of HM^{2+} ions detected in the EU-1 zeolite (4 per unit cell) shows that it is not possible to accommodate them only in the linear channel, because

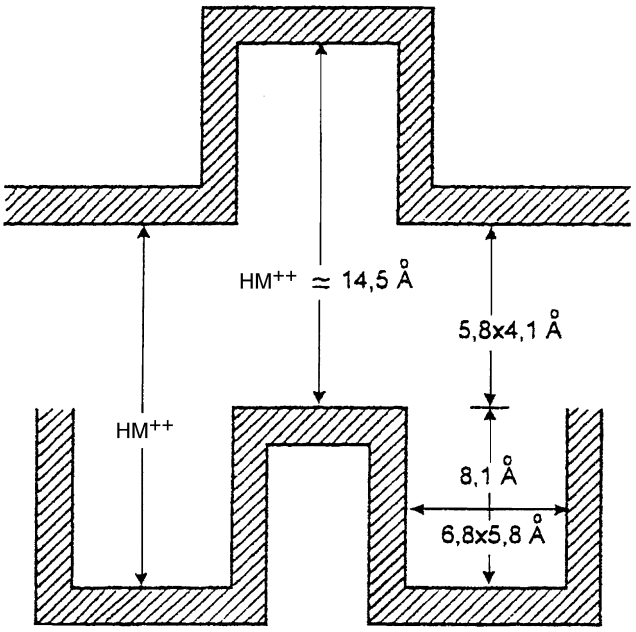

Fig. 5. Schematic representation of HM^{2+} ions in the EU-1 zeolitic channels.

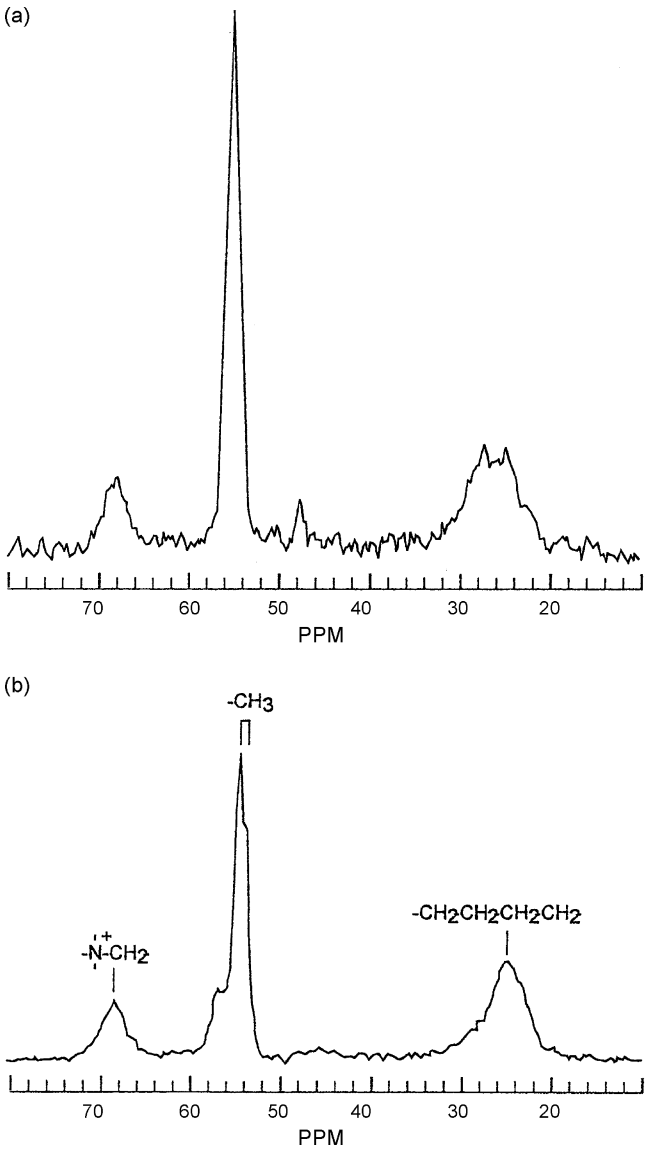

Fig. 6. CP MAS ^{13}C NMR spectrum of hexamethonium ions occluded in EU-1 zeolitic channels (b) and ZSM-48 zeolitic channels (a).

the channel length of one EU-1 unit cell is 27.4 Å [36] and with this assumption the pore filling value would be higher than 100%. The dimensions of EU-1 channel system, that contains a unidimensional 10-membered ring channel (5.8 Å × 4.1 Å), and side pockets (6.8 Å × 5.8 Å in cross-position and 8.1 Å deep) [36] suggest that the hexamethonium can be accommodated in a perpendicular position to the a-axis between the channel and a side-pocket. Following this assumption, it is possible to accommodate 4 HM^{2+} ions into the EUO framework (see Fig. 5) and this hypothesis is in agreement with the value detected for the HM^{2+} ions per unit cell.

X-ray diffraction method and molecular modelling were very successful in positioning the HM^{2+} in the EU-1 channels [37]. The authors showed that the HM^{2+} ions reside in the pockets along the [0 0 1] direction in the EU-1. In order to match the side-pocket, the length of which is equal to 13.9 Å (Fig. 5), the HM^{2+} ions with an estimated length of 14.5 Å in the all-trans confirmation (Table 2) have to adopt gauche confirmation [37].

The MAS ^{13}C NMR spectrum of hexamethonium ions occluded in the EU-1 channels is compared with that of occluded ions in ZSM-48 channels in Fig. 6a and b. Several types of methylene groups can be detected at ca. 25 ppm, in both samples. They are the methylene

groups in the middle of the alkylene chain. The N^+–CH_2 methylene group has its NMR line at 68.2 ppm in EU-1 and 67.9 ppm in ZSM-48. The NMR lines of the CH_3 groups are more informative. Indeed, while the methyl groups of the hexamethonium ions occluded in ZSM-48 are in a quite symmetrical environment (δ = 55.2 ppm) (see Fig. 6a), two different types of methyl groups are identified at 53.8 and 54.7 ppm, respectively for hexamethonium ions occluded in the EU-1 channels (see Fig. 6b). This shows clearly the different chemical environment for the methyl groups. The ^{13}C NMR spectrum is thus in agreement with the model where the HM^{2+} ions are perpendicular to the channel and hence the different carbons experience different chemical environments. Moreover, the hexamethylene chain cannot be in an all-trans conformation because the available space (13.9 Å) is less than the length of the extended molecule (14.5 Å) (Fig. 5). This introduces further variations of the chemical shifts between the various methylene groups of the chain. The study is in progress to identify the various methylene and methyl groups in their correct environment. The ^{13}C NMR values of the HM^{2+} ions incorporated in the EU-1 channels confirm this way the previous results obtained by XRD and molecular modelling [37].

4. Conclusion

The presence of hexamethonium ions in a sodium-aluminosilicate hydrogel, addresses the formation of 5-1 SBU's, favouring the formation of ZSM-48 and EU-1 zeolite. High Si/Al ratios, medium or low OH^-/SiO_2 ratios and OH^-/HM^{2+} ratios between 2.5 and 5 favour the crystallization of ZSM-48 zeolite. By contrast, medium Si/Al ratio close to 25 and a rich sodium and hexamethonium medium, preferentially address the hydrogel to the formation of EU-1 zeolite.

Finally, the hexamethonium ions can accommodate along the ZSM-48 channels (about 1 per unit cell) but they benefit of the side pockets of EU-1 channels for a larger and better accommodation (4 per unit cell).

Acknowledgement

The authors are indebted to Mr. G. Daelen (FUNDP, Namur, Belgium) for his skillful help in taking the NMR spectra.

References

[1] J.L. Casci, B.M. Lowe, T.V. Whittam, British Patent 2,077,709 (1981).
[2] J.L. Casci, B.M. Lowe, T.V. Whittam, US Patent 4,537,754 (1985).
[3] J.L. Casci, Stud. Surf. Sci. Catal. 28 (1986) 215.
[4] A. Moini, K.D. Schmitt, E.W. Valyocsik, R.F. Polomski, Zeolites 14 (1994) 504.
[5] G.H. Kuehl, US Patent 4,482,531 (1984).
[6] J.L. Casci, in: J.B.R. Higgins, von Ballmoos, M.M.J. Treacy (Eds.), Proceedings of the 9th International Zeolite Conference Extended Abstracts, Montreal, 1992, p. A48.
[7] N. Bats, L. Rouleau, P. Caullet, J.L. Paillaud, Y. Mathieu, S. Lacombe, Stud. Surf. Sci. Catal. 154 (2004) 283.
[8] J.L. Casci, A. Stewart, EPA 377 (1990) 291.
[9] M.D. Shannon, J.L. Casci, P.A. Cox, S.J. Andrews, Nature 353 (1991) 417.
[10] A.R. Pradhan, A.N. Kotasthane, B.S. Rao, Appl. Catal. 72 (1991) 311.
[11] F. Di Renzo, G. Giordano, F. Fajula, P. Schulz, D. Anglerot, Patent Appl. FR2698863 (1994), assigned to ELF Aquitaine.
[12] E. Merlen, F. Alario, S. Lacombe, E. Benazzi, J.-F. Joly, C. Ois, US Patent 6,057,486 (2000), assigned to IFP.
[13] L. Rouleau, S. Lacombe, F. Alario, E. Merlen, F. Kolenda, US Patent 6,337,063 (2002), assigned to IFP.
[14] J. Magne-Drisch, J.-F. Joly, E Merlen, F. Alario, US Patent 6,635,791 (2003), assigned to IFP.
[15] R. Millini, F. Frigerio, G. Bellussi, G. Pazzuconi, C. Perego, P. Pollesel, U. Romano, J. Catal. 217 (2003) 298.
[16] W. Souverijns, L. Rombouts, J.A. Martens, P.A. Jacobs, Microporous Mater. 4 (1995) 123.
[17] I. Peral, C.Y. Jones, S.P. Varkey, R.F. Lobo, Microporous Mesoporous Mater. 71 (2004) 125.
[18] A. Dyer, T.I. Emms, J. Mater. Chem. 15 (2005) 5012.
[19] E.B. Webb, G.S. Grest, M. Mondello, J. Phys. Chem. B 103 (1999) 4949.
[20] K.F. Czaplewski, T.L. Reitz, J.K. Yoo, R.Q. Snurr, Microporous Mesoporous Mater. 56 (2002) 55.
[21] See: G. Giordano, Z. Gabelica, N. Dewaele, J.B. Nagy, E.G. Derouane, Stud. Surf. Sci. Catal. 60 (1991) 29, and references cited therein.
[22] G.N. Rao, P.N. Joshi, A.N. Kotasthane, P. Ratnasamy, Zeolites 9 (1989) 483.
[23] S.I. Zones, Zeolites 9 (1989) 458.
[24] X. Wenyang, L. Jianquan, L. Guanghuan, Zeolites 10 (1990) 753.
[25] H. Qisheng, F. Shduhua, X. Ruren, J. Chem. Soc. Chem. Commun. (1988) 1486.
[26] K. Suzuki, Y. Kiyozumi, S. Shin, K. Fujisawa, H. Watanabe, K. Saito, K. Noguchi, Zeolites 6 (1986) 290.
[27] L. Ruifeng, X. Wenyang, W. Jingzhong, Zeolites 12 (1992) 716.
[28] R. Kumar, P. Ratnasamy, Stud. Surf. Sci. Catal. 60 (1991) 43.
[29] G.N. Rao, V.P. Shiralkar, A.N. Kotasthane, P. Ratnasamy, in: M.L. Occelli, H.E. Robson (Eds.), Synthesis of Microporous Materials, Van Nostrand Reinhold, New York, 1992, p. 153.
[30] D.P. Serrano, H.X. Lin, M.E. Davis, J. Chem. Soc. Chem. Commun. (1992) 745.
[31] G. Giordano, N. Dewaele, Z. Gabelica, J.B. Nagy, A. Nastro, R. Aiello, E.G. Derouane, Stud. Surf. Sci. Catal. 69 (1991) 157.
[32] J.B. Nagy, R. Aiello, G. Giordano, A. Katovic, F. Testa, Z. Konya, I. Kiricsi, Mol. Sieves 5 (2007) 365.
[33] G. Giordano, Z. Gabelica, J.B. Nagy, N. Dewaele, E.G. Derouane, in: M.L. Occelli, H.E. Robson (Eds.), Zeolite Synthesis (ACS Symposium Series 398), American Chemical Society, Washington, DC, 1989, p. 587.
[34] G.W. Dodwell, R.P. Denkewicz, L.B. Sand, Zeolites 5 (1985) 153.
[35] J.L. Schlenker, W.J. Rohrbaugh, P. Chu, E.W. Valyocsik, G.T. Kokotailo, Zeolites 5 (1985) 355.
[36] N.A. Briscoe, D.W. Johnson, M.D. Shannon, G.T. Kokotailo, L.B. Mc Cusker, Zeolites 8 (1988) 74.
[37] S.J. Andrews, J.L. Casci, P.A. Cox, M.D. Shannon, in: M.M.J. Treacy, B.K. Marcus, M.E. Bisher, J.B. Higgins (Eds.), Proceedings of the 12th International Zeolite Conference, Materials Research Society, Warrendale, USA, 1999, p. 2355.
[38] W. Inaoka, S. Kasahara, T. Fukushima, K. Igawa, Stud. Surf. Sci. Catal. 60 (1991) 37.